Spectrochimica Acta Part B 88 (2013) 98–103

Contents lists available at ScienceDirect

Spectrochimica Acta Part B

journal homepage: www.elsevier.com/locate/sab

On the determination of plasma electron number density from Stark broadened hydrogen Balmer series lines in Laser-Induced Breakdown Spectroscopy experiments

L. Pardini [a,*], S. Legnaioli [a], G. Lorenzetti [a], V. Palleschi [a], R. Gaudiuso [b], A. De Giacomo [b], D.M. Diaz Pace [c], F. Anabitarte Garcia [d], G. de Holanda Cavalcanti [e], C. Parigger [f]

[a] Istituto di Chimica dei Composti Organometallici del CNR, Area della Ricerca del CNR di Pisa, Via G. Moruzzi 1, 56124 Pisa, Italy
[b] Dipartimento di Chimica, Università di Bari, Via Orabona 4, 70126 Bari, Italy
[c] Instituto de Física 'Arroyo Seco', Facultad de Ciencias Exactas, Paraje Arroyo Seco, B7000GHG Tandil, Argentina
[d] Photonic Engineering Group, Universidad de Cantabria, Edificio I+D+iTelecomunicación, Dpto. TEISA, 39005 Santander, Spain
[e] Institute of Physics, Universidade Federal Fluminense, UFF, Campus da Praia Vermelha, Av. Gal Milton Tavares de Souza, Gragoatá, 24310 240 Niterói, RJ, Brazil
[f] University of Tennessee Space Institute, 411 B. H. Goethert Parkway, Tullahoma, TN 37388-9700, USA

ARTICLE INFO

Article history:
Received 5 November 2012
Accepted 23 May 2013
Available online 10 June 2013

Keywords:
LIBS
Plasma
Hydrogen
Balmer series
Electron density

ABSTRACT

In this work, different theories for the determination of the electron density in Laser-Induced Breakdown Spectroscopy (LIBS) utilizing the emission lines belonging to the hydrogen Balmer series have been investigated. The plasmas were generated by a Nd:Yag laser (1064 nm) pulsed irradiation of pure hydrogen gas at a pressure of $2 \cdot 10^4$ Pa. H_α, H_β, H_γ, H_δ, and H_ε Balmer lines were recorded at different delay times after the laser pulse. The plasma electron density was evaluated through the measurement of the Stark broadenings and the experimental results were compared with the predictions of three theories (the Standard Theory as developed by Kepple and Griem, the Advanced Generalized Theory by Oks et al., and the method discussed by Gigosos et al.) that are commonly employed for plasma diagnostics and that describe LIBS plasmas at different levels of approximations. A simple formula for pure hydrogen plasma in thermal equilibrium was also proposed to infer plasma electron density using the H_α line. The results obtained showed that at high hydrogen concentration, the H_α line is affected by considerable self-absorption. In this case, it is preferable to use the H_β line for a reliable calculation of the electron density.

1. Introduction

Laser-Induced Breakdown Spectroscopy (LIBS) has received recent interest in both basic and applied research, mainly due to its inherent advantages of rapid multi-elemental measurements in solid, liquid, and gaseous samples requiring a minimum preparation [1]. LIBS is based on the spectral analysis of the radiation emitted by a laser-induced plasma (LIP), which can be characterized through determination of its physical parameters, such as temperature, electron density, and atom and ion densities. The most widely used methods for determining the plasma parameters are based on measurement of temperature using the Saha–Boltzmann plot, together with determination of electron density from measurement of Stark broadened spectral lines, utilizing available results for corresponding Stark broadening parameters [2]. Diagnostics of LIPs is of paramount importance in order to get valuable insight about plasma dynamics, with results beneficial for improvement of the LIBS technique in view of analytical applications as well as determination of spectroscopic parameters such as Stark broadening coefficients and transition probabilities [3–15].

Several studies have been devoted to investigate post-breakdown plasma radiation, aimed at matching predictions of theory with experiments [13]. The theory is largely based on the assumption of existence of Local Thermal Equilibrium (LTE) in the measurement time interval (together with the stoichiometry of the ablation process) [1]. A criterion proposed by McWhirter [16], based on the existence of a critical electron density for which the collisions with electrons dominate over the radiative processes, is commonly reported in the literature as a necessary requirement. Thus, a reliable determination of the electron density is critical for evaluation of necessary conditions for establishment of LTE [17].

An illustrative example is the Calibration-Free (CF) LIBS procedure, developed by Ciucci et al. [18,19]. It allows to carry out quantitative analysis without the necessity of constructing calibration curves, provided that lines from all the elements of interest are measured. In the CF-LIBS algorithm, a Saha–Boltzmann plot is employed to evaluate the plasma temperature. The electron density is independently evaluated by measuring the Stark broadening of a suitable line and using coefficients tabulated by Griem [2]. In the case of plasmas generated from

* Corresponding author.
E-mail address: loren.pard@gmail.com (L. Pardini).

0584-8547/$ – see front matter
http://dx.doi.org/10.1016/j.sab.2013.05.030

solid samples in air, the presence of the hydrogen Balmer α line is utilized in the CF-LIBS method. The usefulness of hydrogen Balmer lines for an accurate measurement of electron densities in LIBS plasmas was also demonstrated by El Sherbini et al. [20].

The Stark broadening, in typical LIBS conditions, is the main broadening mechanism of spectral lines [21]. In addition, at a given electron density of the plasma, Stark broadening of hydrogen lines is larger than the one found in atomic lines from other elements [22]. This feature makes the use of hydrogen lines particularly interesting in LIBS experiments with low spectral resolution. Instrumental broadening introduced by the spectrometer might be comparable, or even larger, than the broadening of the emission lines of elements different from hydrogen. Moreover, the Stark broadening of the emission lines is independent from the fulfillment of the LTE conditions, thus making the electron density measurement from Stark broadened lines a very interesting and powerful tool. In recent years, the use of hydrogen Balmer lines has been employed for measurement of temperature and electron density in plasmas generated in gases including several theoretical approximations [23–30].

The aim of the present work is the experimental investigation of different existing theories relevant to LIBS, i.e.: the Standard Theory (ST) as developed by Kepple and Griem [31], the Advanced Generalized Theory (AGT) by Oks et al. [32], and the method discussed by Gigosos et al. (GT) [33], for determination of electron density using lines from the hydrogen Balmer series. To achieve this goal, we studied the temporal evolution of the electron density of plasmas generated in pure hydrogen gas. The experimental results obtained were subsequently compared with the predictions.

2. Theory

2.1. Broadening of spectral lines

The starting point of the three ST, AGT, and GT approaches mentioned in the above section is the normalized line shape indicating the quantum mechanical expression of the energy per unit time of the total system of emitter and perturbers, i.e., the power induced by the dipole operator x_α between an initial higher level i to a final lower level f,

$$L(\omega) = \sum_{\alpha i f} \delta\left(\omega - \omega_{if}^{s}\right) |\langle f | x_\alpha | i \rangle|^2 \rho_i \tag{1}$$

where ρ_i is the probability to find the total system of the perturber and the radiator in the initial state, $\delta(\omega - \omega_{if}^{s})$ is the Dirac Delta distribution, and $L(\omega)$ is the line shape.

In order to find the expression for the line shape, many approximations are needed. This is because the plasma is a very complex system, whose dynamics cannot be exactly described in terms of analytically derived expressions. The usual approach, that is common to all the above-mentioned methods, is to consider only one radiator at a time and to neglect the radiator–radiator interaction. Then, the most demanding task is to model the effect of the surrounding environment, composed of electrons and ions, on the emitting particle. Usually, this effect is separated into two contributions in different frequency regions, since electrons and heavy ions, having different masses, show completely different dynamics. In particular, electrons have a higher mobility, thus resulting in an interaction time with the emitter that is just a fraction of the emitting process; therefore, their influence is treated in the impact approximation [2]. Conversely, ions are treated in the quasi-static approximation [2], since their velocity is low and the effect of the generated electric field is much longer than the duration of the emitting process. This results in Stark-broadening of the lines, i.e., for a given perturber distribution, corrections to ω_{if}^{s} due to the ion microfield are calculated within time-independent perturbation theory.

Additionally, the no-quenching approximation is used. It means that the effects of the perturbers will not mix the emitter quantum states with different principal quantum numbers. As a consequence, no quadratic or higher order Stark effect can be described by these models, thus limiting their applicability to not-too-high electron densities (i.e., lower than 10^{20} cm^{-3}). Taking into account the above-mentioned approximations, one finds the following formula that is commonly used in ST as well as in AGT:

$$L(\omega) = \frac{1}{\pi} Re\left[Tr \int_0^\infty d\mathrm{F}\, \mathrm{W(F)}\, \mathrm{D}\left[i(\omega - \omega(\mathrm{F})) + \Phi(\mathrm{F})\right]^{-1}\right] \tag{2}$$

where F is the ion field, D the dipole–dipole operator, Φ(F) the impact operator and W(F) the ion micro-field distribution function.

The differences between ST and AGT approaches arise after this step: AGT treats one of the components of the electric field **E** generated by electrons in a non-perturbative way (in particular the component which lies along the electric field generated by ions), whereas in ST all the components of **E** are treated perturbatively. However, both theories can describe certain experiments in a satisfactory way, although the contribution of the ion dynamics is not taken into account in both of them.

The method proposed by Gigosos (GT), in turn, takes into account the ion dynamics, so this theory should be, at least in principle, more accurate. In this approach, plasma is considered to be weakly-coupled, globally neutral, homogeneous and isotropic and the perturbing particles are treated as classical particles moving along straight trajectories with constant velocity. The interaction between particles is neglected and it is accounted for ad hoc by adopting a Debye screened potential.

2.2. Spectral line emission from a homogeneous plasma in LTE

The integrated wavelength-dependent spectral intensity of a self-absorbed line $\overline{I_{SA}}$ emitted from a pure hydrogen homogeneous plasma in LTE along the line-of-sight is given by [34]:

$$\overline{I_{SA}} = \overline{I_0}\left(\frac{1 - e^{-\tau(\lambda_0)}}{\tau(\lambda_0)}\right)^{0.46} = (SA)^{0.46} \tag{3}$$

where $\tau(\lambda_0) = \tau_0$ (dimensionless) is the wavelength-dependent optical thickness [8]. Optically thin plasma condition is therefore achieved for $\tau(\lambda)$ approaching zero. In Eq. 3, the ratio between H_α and H_β line intensities can be thus written as:

$$\frac{\overline{I_\alpha}}{\overline{I_\beta}} \Big/ \frac{\overline{I_{\alpha_0}}}{\overline{I_{\beta_0}}} = (SA)^{0.46}. \tag{4}$$

By comparing the experimental values of the $\frac{\overline{I_\alpha}}{\overline{I_\beta}}$ ratio with the theoretical ones of $\frac{\overline{I_{\alpha_0}}}{\overline{I_{\beta_0}}}$ without self-absorption, τ_0 can be estimated. Considering the data reported in the following sections (see Fig. 6), the ratio in the left-hand side of Eq. 4 is about 0.35, from which we find the estimated value for the optical thickness $\tau_0 \cong 10$.

3. Experimental arrangement

The experimental arrangement as well as the main measured features of the temporal trend of the hydrogen-spectrum has been discussed previously [35]. The experimental arrangement consists of a Nd:YAG laser source operating at 1–20 Hz, 7 ns pulse duration at 1064 nm, a monochromator (TRIAX 550 Jobin Yvon with 150 g/mm grating) connected to an ICCD (i3000 Jobin Yvon) and a pulse generator (Stanford Inc. DG 535) that we used for controlling delay time and detector gate width. The vacuum chamber is a typical Pulsed Laser Deposition (PLD) reactor, equipped with several windows for entrance of the laser radiation, and detection of the emission

spectrum and pressure gage. The chamber is evacuated by a turbomolecular pump coupled with a rotary pump; the pressure inside the chamber is controlled by two dosing valves and a fluxmeter. Pure hydrogen gas at $2 \cdot 10^4$ Pa has been irradiated with a laser pulse of energy 800 mJ, and repetition rate 20 Hz, focused in the vacuum chamber by a 30 cm focal length lens. The plasma light generated in the vacuum chamber is imaged by a 7.5 cm focal length biconvex lens on the aperture of a fused silica optical fiber. The acquisition was not spatially resolved, therefore no Abel inversion was performed on the spectra. The spectra have been collected in the time range from 250 ns to 1000 ns after the laser pulse at intervals of 50 ns, with a gate width of 50 ns. The spectral response as well as the radiometric response of the detection system has been calibrated with certified lamps.

4. Results and discussion

Fig. 1 shows a typical, original LIBS spectrum recorded following laser-induced breakdown in pure hydrogen, covering the spectral range from 276 to 683 nm, where the stronger emissions belonging to the H Balmer series are clearly observed. The spectral lines H_α, H_β, H_γ, H_δ, and H_ε, marked in the spectrum, were selected for the present analysis and their intensities were corrected taking into account the spectral sensitivity of the acquisition system. These lines are isolated and practically free from interference so they are suitable for plasma characterization. With this aim, LIBS spectra were acquired in the time interval between 200 and 950 ns after the laser pulse at intervals of 50 ns (gate time = 50 ns).

It is worth noting that the possibility of detecting the lines of the Hydrogen Balmer series in the spectrum is described by the Inglis–Teller equation [36]. According to this equation, the maximum value of n_e for detection of the H_ε line should be, in the experimental conditions of this work, $n_e = 0.7 \cdot 10^{17}$ cm^{-3}. The electron number density, estimated from the H_β Stark broadening, is $n_e = 1.1 \pm 0.2 \cdot 10^{17}$ cm^{-3} at a delay of 200 ns immediately after the onset of the laser plasma and decreases below the Inglis–Teller limit at delays between 250 and 300 ns (see Fig. 4). Considering the indetermination in both the theoretical model and the experimental results, the Inglis–Teller equation thus explains the presence of the H_ε line in our spectra and excludes the practical possibility of detecting the H_ζ line (388.90 nm) whose Inglis–Teller limiting value is $n_e = 0.3 \cdot 10^{17}$ cm^{-3}. In our experiment the electron number density, estimated from the H_β Stark broadening, goes below this threshold only for delays greater than 500 ns, i.e. when the intensity of the H_ζ line already dropped below the quantitation limit of our system.

The electron temperature of the plasma at each delay time was evaluated using the Boltzmann plot method with H_α, H_β, and H_γ lines. Fig. 2 shows results of these calculations. The calculation of the electron temperature was performed as a check that the experimental conditions would not vary too much while varying the acquisition delay. In fact, the dependence on the plasma temperature of the theoretical parameters used for deriving the electron number density is very weak. A more precise determination of the electron temperature should have taken into account, and been corrected for, the effects of self-absorption. The error bars correspond to the typical uncertainty of temperature measurements. It can be seen that the temperature decreases with time due to plasma cooling. Despite the fact that the values show a slight dispersion, the order of magnitude of the temperature is well defined, ranging between 8000 K and 13,000 K for the time interval analyzed.

The plasma electron density was calculated through the Lorentzian Stark broadenings (w_L) of the H Balmer lines using the measured Full-Widths at Half-Maximum (FWHM). Since the spectra were obtained using a spectrometer with low spectral resolution, the Gaussian contribution to the line broadening (w_G) is mainly given by the instrumental profile. The instrumental width was evaluated by measuring the FWHM of the two most intense lines of a Kr-ion laser whose spectrum was acquired in the same conditions as our main experiment. The width of these lines was about 13 Å. The Doppler line width, estimated from the plasma temperature, is negligible with respect to the instrumental width in the time windows considered. Then, the instrumental width was discounted from the total measured widths (w_{tot}), by using the Voigt formula [37]:

$$w_L = w_{tot} - w_G^2 / w_{tot}. \quad (5)$$

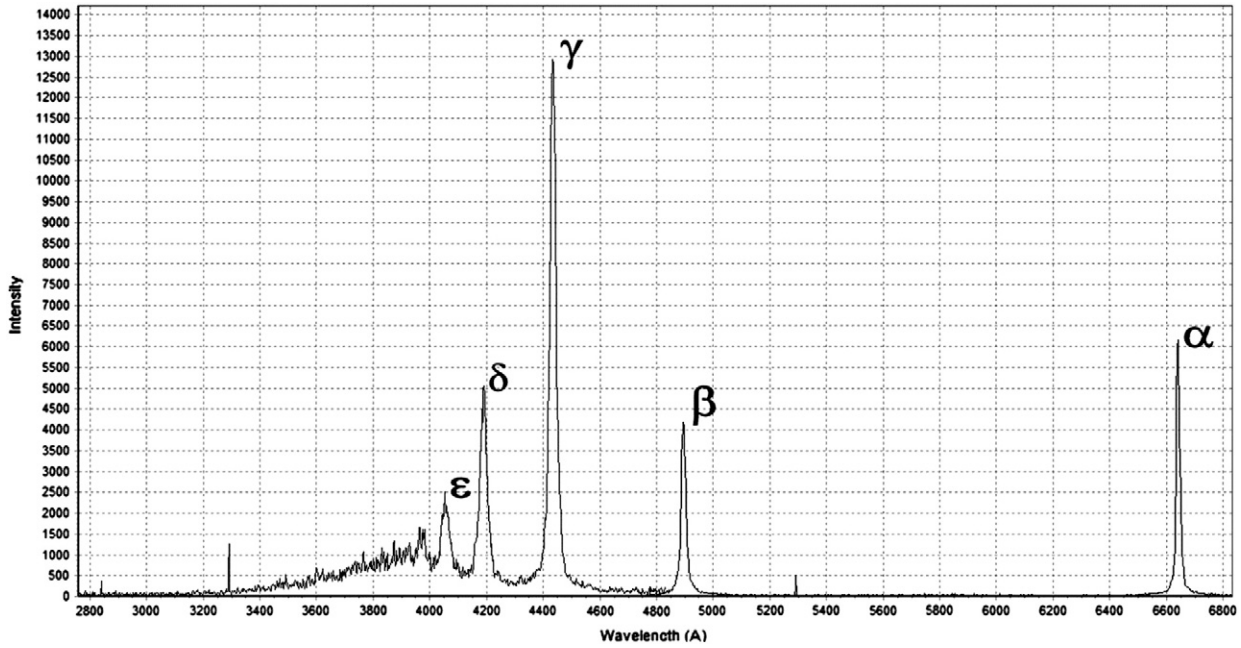

Fig. 1. LIBS spectrum of the emission from a plasma generated from pure hydrogen at $2 \cdot 10^4$ Pa; the spectrum shown is not corrected for the sensitivity of the detector system. Acquisition parameters are: Nd:YAG laser source operating at 1064 nm, 7 ns pulse duration, 800 ns acquisition delay, 50 ns acquisition gate. H Balmer lines used in this work are indicated in the spectrum.

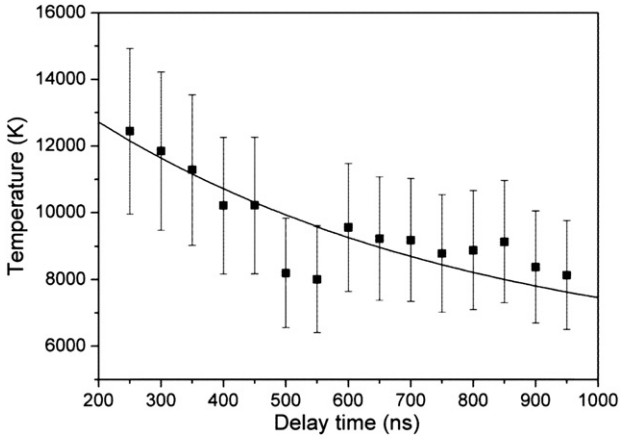

Fig. 2. Temporal evolution of the plasma temperature.

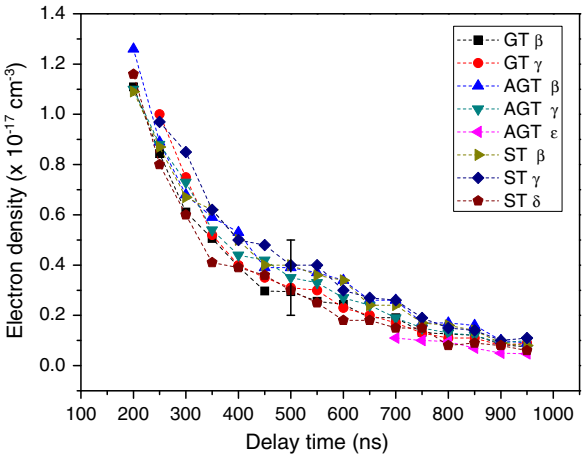

Fig. 3. Electron density from Balmer H_β, H_γ, H_δ, and H_ε lines according to the ST, AGT, and GT. For clarity, the error bar is indicated for only the 500 ns delay data.

The effective Stark broadenings obtained are reported in Table 1 for the different spectral lines and delay times.

Starting from the Stark widths listed in Table 1, we applied the three ST, AGT, and GT approaches described in Section 2.1 for calculating the plasma electron density. Namely:

(i). ST: Tables compiled by Kepple and Griem, in which the broadenings are reported as a function of temperature and electron density for the Balmer lines H_α, H_β, H_γ, and H_δ.
(ii). AGT: Tables compiled by Oks et al., in which the broadenings are reported as a function of temperature and electron density for the Balmer lines H_α, H_β, H_γ, H_δ, and H_ε.
(iii). GT: Graphs obtained by Gigosos et al., which take into account the ion dynamics and their masses; in the graphs, the curves are reported as a function of temperature and electron density for the Balmer lines H_α, H_β, and H_γ.

The electron densities calculated from all the H Balmer lines should be the same, within experimental errors. As can be seen in Fig. 3, the values derived from the lines H_β and H_γ (and H_ε for the few accessible points) are essentially the same for all the approaches, within reproducibility of the measurements.

The error bar reported represents the variability among the electron densities calculated for the different lines according to the corresponding theoretical frameworks. In turn, Fig. 4 shows that the values derived from AGT for the H_δ line are lower than those obtained with GT. No data are available at this time for H_δ from GT; however, values calculated from the H_β line from GT was selected for comparisons. The error bar represents, as in Fig. 3, the variability among the electron densities calculated according to the different theories. Similarly, it seems that all the proposed approaches fail in the case of H_α line, as observed in Fig. 5. Besides showing the fact that self-absorption is affecting the determination of electron density from the H_α line, it is also worth noting in the figure that the different theoretical approaches give very different evaluations of the electron density, starting from the same experimentally determined line broadening. The observed discrepancies indicate a range from a factor of 3 for AGT to less than 2 for GT.

Since our LIBS experiment was performed in pure hydrogen, the reason for the discrepancy can be likely related to the occurrence of self-absorption, as also suggested in other works [30]. To evaluate a possible self-absorption of the stronger H Balmer lines, we compared the experimental intensity ratios of the lines H_α and H_β with the theoretical values expected in optically thin conditions, according to the equation:

$$\frac{I_\alpha}{I_\beta} = \frac{A_{ij}^\alpha}{A_{ij}^\beta} e^{\left(-\frac{E_{j,\alpha}-E_{j,\beta}}{kT}\right)} \quad (6)$$

where the superscripts α and β refer to H_α and H_β, respectively. Fig. 6 illustrates the comparison of the experimental ratios with the ratios calculated for each delay time.

A reduction in the experimental ratio of the strongest line (H_α) relative to the weaker line (H_β) is clearly observed. This trend indicates that the H_α line suffers a considerable self-absorption in the

Table 1
Plasma electron temperature (in K) and FWHM (in Å) of Balmer lines H_α to H_ε at different acquisition delays.

Delay (ns)	T (K)	H_α	H_β	H_γ	H_δ	H_ε
200	–	17.0	51.5	69.8	92.0	–
250	12,400	15.0	42.8	55.2	74.8	–
300	11,900	12.5	34.3	47.5	58.1	–
350	11,300	10.1	30.2	36.5	44.6	–
400	10,200	9.4	25.4	30.6	42.2	–
450	10,200	8.6	21.0	29.1	40.7	–
500	8100	7.7	20.9	25.5	35.2	–
550	8000	6.1	19.0	25.1	32.0	–
600	9500	5.9	18.4	21.2	27.1	–
650	9200	6.4	15.5	19.0	27.2	–
700	9200	4.8	15.5	18.0	24.1	32.4
750	8800	4.9	12.1	15.3	25.1	29.0
800	8900	4.9	11.7	13.6	18.5	26.1
850	9100	3.2	11.4	13.1	20.0	23.3
900	8400	2.7	8.9	11.8	16.7	19.0
950	8100	3.9	8.2	12.0	14.6	15.5

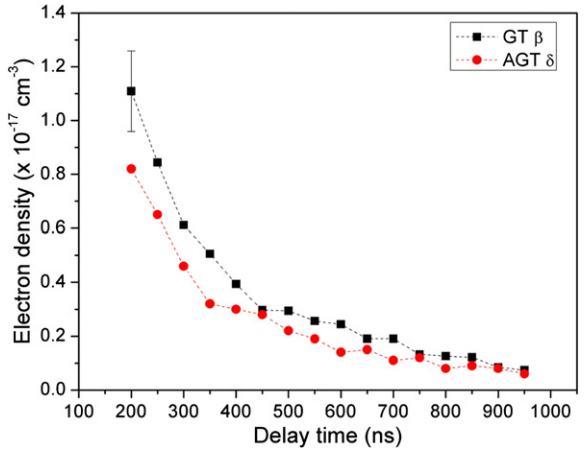

Fig. 4. Electron density from Balmer H_β and H_δ lines according to GT and AGT.

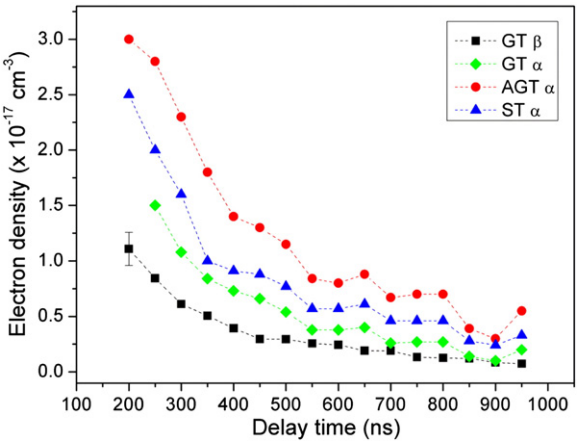

Fig. 5. Electron density from Balmer H_α line according to GT, AGT, and ST; values derived from GT H_β are reported as reference.

time interval observed. Thus, for our experimental conditions, self-absorption originates an apparent broadening of this line [8] that causes an overestimation of the actual electron density (compare Fig. 1) so it cannot be used for a reliable determination of the electron density.

Note that the Gigosos approach is generally applicable in the analysis of LIBS spectra because it takes into account the ion dynamics, while the other two approaches do not. The relevant results are presented in graphical form, so the use of the GT data cannot be implemented immediately, especially when calculation of electron density is performed in analytical, automated computer software [38]. Hence, in order to ease the use of GT results, we derived an empirical relation linking the Stark FWHM of the Balmer H_α line with the plasma electron density, in the form:

$$n_e = 8.02 \cdot 10^{12} \left(\frac{\mathrm{FWHM}}{\alpha} \right)^{3/2} \tag{7}$$

where

$$\alpha = \frac{1}{a + b/\sqrt{n_e}} \tag{8}$$

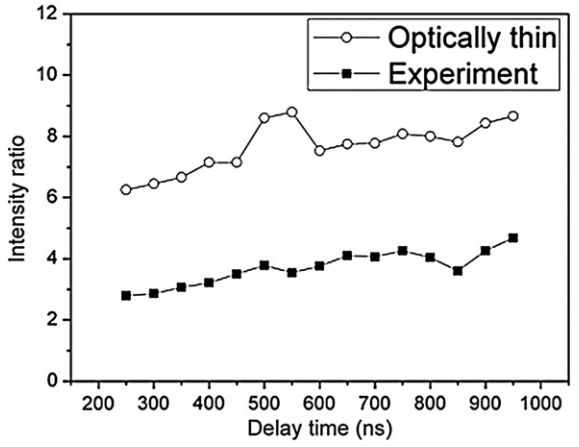

Fig. 6. Experimental (black squares) and theoretical (circles) intensity ratios of the H_α line with respect to the H_β line for different acquisition delays.

with:

$$a = \sqrt{4033.8 - 24.45 \cdot (\ln T)^2}$$
$$b = 1.028 \cdot 10^9 + 174576.3 \cdot T. \tag{9}$$

This expression reproduces the Gigosos tabulated data within a 5% accuracy in typical LIBS conditions. For the Balmer H_β line, in turn, Gigosos proposed the formula linking the FWHM to electron density [33]:

$$\mathrm{FWHM}_\beta = 4800 \cdot \left(n_e \cdot 10^{-17} \mathrm{cm}^3 \right)^{0.68116}. \tag{10}$$

5. Conclusions

Time-resolved LIBS measurements were reported in pure hydrogen at the pressure of $2 \cdot 10^4$ Pa. The plasma electron density was derived using different theories proposed by Kepple and Griem, by Oks et al. and by Gigosos et al. from the measured Stark broadening of the most intense H Balmer emission lines, i.e.: H_α to H_ε, recorded at different delay times following generation of laser-induced plasma. The values of the electron density obtained were compared and the observed discrepancies were interpreted in terms of plasma self-absorption of the Balmer H_α line, the most intense of the series. When the hydrogen concentration is low enough for the Balmer alpha line to be optically thin, as reported in literature [28], the theoretical treatment proposed by Gigosos would be in principle preferred, given the fact that this approach starts from the same approximations of the Griem and Oks theories but considers, in the theoretical treatment, also the effect of the ion dynamics. However, a deep understanding of the true advantages of this approach was not the aim of this work, but they should be definitely proven with further experiments. Conversely, when the H concentration is high for self-absorption of the H_α line to occur, we found that the most suitable line to infer the electron density is the H_β line. In this case, the analysis of the Stark width should be treated according to the Gigosos approximation, which gives equivalent results with respect to ST and AGT theories. GT shows a further advantage of being easily put in analytical, although empirical, form. When the use of the H_α line is feasible, in view of easing the application of the methods to the automatic calculation of electron density in analytical software, we also derived an empirical expression that practically gives the same results.

Acknowledgment

The authors acknowledge the useful discussions with Prof. Nicolò Omenetto, University of Florida, Gainesville.

Lorenzo Pardini acknowledges the support of the European Commission, of the Italian Ministero del Lavoro, della Salute e delle Politiche Sociali and of Regione Toscana, through the POR FSE 2007–2013 'MONDI' grant. Diego M. Diaz Pace acknowledges the support of the Concejo Nacional de Investigationes Científicas y Técnicas (CONICET) of Argentina. Francisco Anabitarte Garcia acknowledges the support of the grant AP2007-02230 from the Spanish Government. Gildo de Hollanda Cavalcanti acknowledges the support of CAPES (Coordenadoria de Aperfeiçoamento de Pessoal do Ensino Superior), proc.3877-11-6, for the financial support.

References

[1] A.W. Miziolek, V. Palleschi, I. Schechter, Laser Induced Breakdown Spectroscopy, Cambridge University Press, 2006.
[2] H.R. Griem, Spectral Line Broadening by Plasmas, Academic Press, New York, NY, USA, 1974.
[3] C. Aragón, J.A. Aguilera, Characterization of laser induced plasmas by optical emission spectroscopy: a review of experiments and methods, Spectrochim. Acta, Part B 63 (2008) 893–916.

[4] N. Konjević, M. Ivković, S. Jovićević, Spectroscopic diagnostics of laser-induced plasmas, Spectrochim. Acta, Part B 65 (2010) 593–602.
[5] C. Aragón, J. Bengoechea, J.A. Aguilera, Asymmetric Stark broadening of the Fe I 538.34 nm emission line in a laser induced plasma, Spectrochim. Acta, Part B 60 (2005) 897–904.
[6] J. Bengoechea, J.A. Aguilera, C. Aragón, Application of laser-induced plasma spectroscopy to the measurement of Stark broadening parameters, Spectrochim. Acta, Part B 61 (2006) 69–80.
[7] C. Colón, A. Alonso-Medina, Application of a laser produced plasma: experimental Stark widths of single ionized lead lines, Spectrochim. Acta, Part B 61 (2006) 856–863.
[8] F. Bredice, F.O. Borges, H. Sobral, M. Villagran-Muniz, H.O. Di Rocco, G. Cristoforetti, S. Legnaioli, V. Palleschi, A. Salvetti, E. Tognoni, Measurement of Stark broadening of Mn I and Mn II spectral lines in plasmas used for Laser-Induced Breakdown Spectroscopy, Spectrochim. Acta, Part B 62 (2007) 1237–1245.
[9] J. Manrique, J.A. Aguilera, C. Aragón, Determination of transition probabilities by laser-induced breakdown spectroscopy with curve-of-growth measurements, J. Quant. Spectrosc. Radiat. Transfer 112 (2011) 85–91.
[10] Alonso-Medina, A spectroscopic study of laser-induced tin–lead plasma: transition probabilities for spectral lines of Sn I, Spectrochim. Acta, Part B 65 (2010) 158–166.
[11] P. Matheron, A. Escarguel, R. Redon, A. Lesage, J. Richou, Si II transition probabilities measurements in a laser induced plasma, J. Quant. Spectrosc. Radiat. Transfer 69 (2001) 535–541.
[12] A. Alonso-Medina, C. Colón, C. Herrán-Martinez, Experimentally determined transition probabilities for lines of Pb I and the 2203.5 Å line of Pb II, J. Quant. Spectrosc. Radiat. Transfer 68 (2001) 351–362.
[13] A. De Giacomo, A novel approach to elemental analysis by Laser Induced Breakdown Spectroscopy based on direct correlation between the electron impact excitation cross section and the optical emission intensity, Spectrochim. Acta, Part B 66 (2011) 661–670.
[14] I.B. Gornushkin, U. Panne, Radiative models of laser-induced plasma and pump-probe diagnostics relevant to laser-induced breakdown spectroscopy, Spectrochim. Acta, Part B 65 (2010) 345–359.
[15] D. Pietanza, G. Colonna, A. De Giacomo, M. Capitelli, Kinetic processes for laser induced plasma diagnostic: a collisional-radiative model approach, Spectrochim. Acta, Part B 65 (2010) 616–626.
[16] R.W.P. McWhirter, in: R.H. Huddlestone, S.L. Leonard (Eds.), Plasma Diagnostic Techniques, Academic Press, New York, 1965, pp. 201–264, (Chapter 5).
[17] G. Cristoforetti, A. De Giacomo, M. Dell'Aglio, S. Legnaioli, E. Tognoni, V. Palleschi, N. Omenetto, Local thermodynamic equilibrium in laser-induced breakdown spectroscopy: beyond the McWhirter criterion, Spectrochim. Acta, Part B 65 (2010) 86–95.
[18] E. Tognoni, G. Cristoforetti, S. Legnaioli, V. Palleschi, Calibration-free laser-induced breakdown spectroscopy: state of the art, Spectrochim. Acta, Part B 65 (2010) 1–14.
[19] A. Ciucci, M. Corsi, V. Palleschi, S. Rastelli, A. Salvetti, E. Tognoni, New procedure for quantitative elemental analysis by laser-induced plasma spectroscopy, Appl. Spectrosc. 53 (8) (1999) 960–964.
[20] A.M. El Sherbini, H. Hegazy, Th.M. El Sherbini, Measurement of electron density utilizing the Hα-line from laser produced plasma in air, Spectrochim. Acta, Part B 61 (2006) 532–539.
[21] H.R. Griem, Plasma Spectroscopy, McGraw-Hill, New York, 1964.
[22] S. Alexiou, Overview of plasma line broadening, High Energy Density Phys. 5 (2009) 225–233.
[23] C.G. Parigger, M. Dackman, J.O. Hornkohl, Time-resolved spectroscopy measurements of hydrogen-alpha, -beta, and -gamma emissions, Appl. Opt. 47 (2008) G1–G6.
[24] J.B. Simeonsson, L.J. Williamson, Characterization of laser induced breakdown plasmas used for measurements of arsenic, antimony and selenium hydrides, Spectrochim. Acta, B 66 (2011) 754–760.
[25] R. Zikić, M.A. Gigosos, M. Ivković, M.A. González, N. Konjević, A program for the evaluation of electron number density from experimental hydrogen Balmer beta line profiles, Spectrochimica. Acta, Part B 57 (2002) 987–998.
[26] C. Parigger, Diagnostic of a laser-induced optical breakdown based on half-width at half area of H_α, H_β, and H_γ lines, Int. Rev. At. Mol. Phys. (IRAMP) 1 (2010) 129–136.
[27] C. Parigger, E. Oks, Hydrogen Balmer series spectroscopy in laser-induced breakdown plasmas, Int. Rev. At. Mol. Phys. (IRAMP) 1 (2010) 13–23.
[28] C. Aragón, J.A. Aguilera, Determination of the local electron number density in laser-induced plasmas by Stark-broadened profiles of spectral lines: comparative results from H_α, Fe I and Si II lines, Spectrochim. Acta, Part B 65 (2010) 395–400.
[29] E. Tognoni, M. Hidalgo, A. Canals, Combination of the ionic-to-atomic line intensity ratios from two test elements for the diagnostic of plasma temperature and electron number density in inductively coupled plasma atomic emission spectroscopy, Spectrochim. Acta, Part B 62 (2007) 435–443.
[30] C.G. Parigger, D.H. Plemmons, E. Oks, Balmer series H measurements in a laser-induced hydrogen plasma, Appl. Opt. 42 (2003) 5992–6000.
[31] P. Kepple, H.R. Griem, Improved stark profile calculations for the hydrogen lines Hα, Hβ, Hγ, and Hδ, Phys. Rev. 173 (1968) 317–325.
[32] J. Touma, E.A. Oks, S. Alexiou, A. Derevianko, Review of the advanced generalized theory for Stark broadening of hydrogen lines in plasmas with tables, J. Quant. Spectrosc. Radiat. Transfer 65 (2000) 543–571.
[33] M.A. Gigosos, M.A. Gonzalez, V. Cardenoso, Computer simulated Balmer-alpha, -beta and -gamma Stark line profiles for non-equilibrium plasmas diagnostics, Spectrochim. Acta, Part B 58 (2003) 1489–1504.
[34] A.M. El Sherbini, T.M. El Sherbini, H. Hegazy, G. Cristoforetti, S. Legnaioli, V. Palleschi, L. Pardini, A. Salvetti, E. Tognoni, Evaluation of self-absorption coefficients of aluminum emission lines in laser-induced breakdown spectroscopy measurements, Spectrochim. Acta, Part B 60 (2005) 1573–1579.
[35] A. De Giacomo, R. Gaudiuso, M. Dell'Aglio, A. Santagata, The role of continuum radiation in laser induced plasma spectroscopy, Spectrochim. Acta, Part B 65 (2010) 385–394.
[36] D.R. Inglis, E. Teller, Ionic depression of series limits in one-electron spectra, Astrophys. J. 90 (1939) 439–448.
[37] M. Danos, S. Geschwind, Broadening of microwave absorption lines due to wall collisions, Phys. Rev. 91 (1953) 1159–1162.
[38] E. Tognoni, G. Cristoforetti, S. Legnaioli, V. Palleschi, A. Salvetti, M. Mueller, U. Panne, I. Gornushkin, A numerical study of expected accuracy and precision in Calibration-Free Laser-Induced Breakdown Spectroscopy in the assumption of ideal analytical plasma, Spectrochim. Acta, Part B 62 (2007) 1287–1302.